Bioorganic Chemistry 91 (2019) 103124

Contents lists available at ScienceDirect

Bioorganic Chemistry

journal homepage: www.elsevier.com/locate/bioorg

Flavonols and 4-thioflavonols as potential acetylcholinesterase and butyrylcholinesterase inhibitors: Synthesis, structure-activity relationship and molecular docking studies

Ehsan Ullah Mughal[a,*], Amina Sadiq[b,*], Jamshaid Ashraf[a], Muhammad Naveed Zafar[c], Sajjad Hussain Sumrra[a], Rubina Tariq[b], Amara Mumtaz[d], Asif Javid[a], Bilal Ahmad Khan[e], Anser Ali[f], Chaudhary Omer Javed[b]

[a] Department of Chemistry, University of Gujrat, Gujrat 50700, Pakistan
[b] Department of Chemistry, Govt. College Women University, Sialkot 51300, Pakistan
[c] Department of Chemistry, Quaid-i-Azam University, Islamabad 45320, Pakistan
[d] Department of Chemistry, COMSATS University Islamabad, Abbottabad Campus 22060, Pakistan
[e] Department of Chemistry, University of Azad Jammu and Kashmir, Muzaffarabad, Pakistan
[f] Department of Zoology, Mirpur University of Science and Technology, Mirpur 10250, Pakistan

ARTICLE INFO

Keywords:
Flavonoids
Flavonols
3-hydroxyflavones
4-thioflavonols
Sulfur compounds
Cholinesterases
AChE/BChE inhibitors
Molecular docking studies

ABSTRACT

To explore new scaffolds for the treat of Alzheimer's disease appears to be an inspiring goal. In this context, a series of varyingly substituted flavonols and 4-thioflavonols have been designed and synthesized efficiently. All the newly synthesized compounds were characterized unambiguously by common spectroscopic techniques (IR, ^{1}H-, ^{13}C NMR) and mass spectrometry (EI-MS). All the derivatives (**1–24**) were evaluated *in vitro* for their inhibitory potential against cholinesterase enzymes. The results exhibited that these derivatives were potent selective inhibitors of acetylcholinesterase (AChE), except the compound **11** which was selective inhibitor of butyrylcholinesterase (BChE), with varying degree of IC_{50} values. Remarkably, the compounds **20** and **23** have been found the most potent almost dual inhibitors of AChE and BChE amongst the series with IC_{50} values even less than the standard drug. The experimental results *in silico* were further validated by molecular docking studies in order to find their binding modes with the active pockets of AChE and BChE enzymes.

1. Introduction

Flavonols (Fig. 1) are one of the significant subclasses of flavonoids and have been extensively studied for their antioxidant properties in the food and health sciences [1–3]. They are ubiquitously distributed in plants with a wide range of biological and pharmacological activities such as antifungal, antimicrobial, neuroprotective, antioxidant, HIV-inhibitory and anticancer activities [4–6]. However, these compounds are found naturally in limited amounts. Therefore, there is need of the hour to find chemical pathways for the synthesis of analogues of such significant structures in large amounts in order to cope with new challenges in medicinal chemistry.

Moreover, sulfur containing compounds usually possess good biological activities, which can be speculated by their ability to scavenge free radicals, high potential of chelating metal cations and capacity of affecting key redox enzymes [7]. Interestingly, recent studied have emphasized that sulfur containing small molecules and enzymes played a key role in a wide range of fundamental biological functions, which intensely attracted many researchers to develop new thio-compounds in disease therapy and prevention [8]. In this context, 4-thioflavonols (Fig. 1) and their derivatives have been reported to possess potent biological properties such as anticancer, antimicrobial and green pesticides etc. [9–11]. However, despite the fact that the conversion of the carbonyl (C═O) group in 2-phenylchromone framework into thiocarbonyl (C═S) group has been usually described as a feasible strategy [8,12], the inhibitory potential against cholinesterase enzymes of sulfur-containing flavonols have been much less reported.

Alzheimer's disease (AD) which is characterized by the B-amyloid plaque formation or neuromediator acetylcholine deficiency is a neurodegenerative disease and is one of the most frequent forms of dementia and has become one of the serious halt problem among the elderly people [13–15]. The acetylcholinesterase (AChE) and

* Corresponding authors.
E-mail addresses: ehsan.ullah@uog.edu.pk (E.U. Mughal), amina.sadiq@gcwus.edu.pk (A. Sadiq).

https://doi.org/10.1016/j.bioorg.2019.103124
Received 9 May 2019; Received in revised form 4 July 2019; Accepted 11 July 2019
Available online 12 July 2019

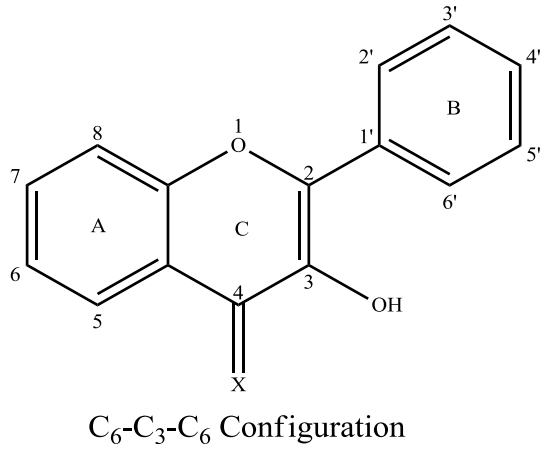

Fig. 1. Representative structures of flavonol (X = O) and 4-thioflavonol (X = S).

butyrylcholinesterase (BChE) enzymes have been documented as critical targets for the effective management of AD by an increase in the availability of acetylcholine in the brain regions and decrease in the Ab deposition because both of these enzymes play an important role in Ab-aggregation during the early stages of senile plaque formation [16]. Although a large number of AChE and BChE inhibitors have been reported in literature [17], but these inhibitors still have possible side effects and bioavailability problems, due to which there is still great interest in finding better AChE and BChE inhibitors. Recently the flavonoids are prescribed acetylcholinesterase inhibitor as they have the advantages of been more tolerable, cheaper and easy natural occurrence [18,19]. However, the role of synthetic flavanols and 4-thioflavonols as potential cholinesterase inhibitors remains an interesting goal and a constant endeavor. These compounds could thus be appeared as promising lead structures for the development of new scaffolds for the treatment of Alzheimer's disease.

Owing to the potential pharmacological applications and much less synthetic work on these compounds have enforced us to synthesize these novel compounds and also to evaluate their role as cholinesterase enzymes inhibitors. In addition, because of the significant relevance of flavonol derivatives in medicinal chemistry and our continuous quest to develop potent cholinesterase inhibitors, we aimed to explore the cholinesterase inhibition potential of flavonols and 4-thioflavonols, which to the best of our knowledge have not been reported so far. Moreover, it is also desire to study the effect of replacing oxygen with sulfur and various substituents on cholinesterase inhibitory potential of these compounds, and to establish the structure activity relationship (SAR) for each of the synthesized compound. The experimental results have also been validated by molecular docking studies.

2. Material and methods

All the chemicals were purchased from Merck (Germany) and Sigma-Aldrich (USA) and used as delivered. Melting points were measured on an Electrothermal melting point apparatus and are uncorrected. The IR spectra were recorded on a Bio-red spectrophotometer. NMR spectra were measured on a Bruker DRX 300 instrument (^{1}H, 500 MHz, ^{13}C, 125 MHz). Accurate mass measurements were carried out with the Fisons VG sector-field instrument (EI) and a FT-ICR mass spectrometer. The IR values are mentioned in $\bar{\upsilon}$ units and NMR chemical shift values were determined in ppm units. Absorption spectra were recorded in dichloromethane on Jasco UV–VIS V-660 or Jasco UV–VIS V-670 instrument.

2.1. General procedure for the synthesis of flavonols and 4-thioflavonols

A mixture of 2-hydroxyacetophenone (1.2 mL, 10.0 mmol) and 10.0 mL aqueous solution of sodium hydroxide (30%) was stirred for 30 min in methanol (15.0 mL) followed by the addition of benzaldehyde (1.0 mL, 10.0 mmol), and the reaction mixture was further stirred for 4 h at ambient temperature. The progress of the formation of 2-hydroxychalcone was monitored by comparative TLC. Chalcone formed, *in situ*, was further cyclized by adding 1.5 mL hydrogen peroxide solution (35%) in the same reaction mixture (without isolating it from the reaction mixture) and allowed it to stir for further 1–2 h. After completion of the reaction (checked by TLC), HCl (10%) was added to the reaction mixture in order to neutralize it. As a result, precipitates of flavonol were formed. These precipitate were filtered through Buchner funnel followed by washing with a plenty of water. The residue obtained was then dried and recrystallized by ethanol. To a solution of simple flavonol (238.23 mg, 1.0 mmol) in anhydrous toluene (10.0 mL) was added Lawesson's reagent (485.37 mg, 1.2 mmol), producing a turbid yellow color, and the reaction mixture was heated to reflux (120–125 °C) for 20 h (monitored the reaction by TLC) under an argon atmosphere. The reaction mixture was protected from light with aluminum foil. After the completion of reaction, the resulting red-brown solution was filtered under vacuum to remove insoluble impurities, and the filtrate was evaporated to dryness on a rotorary evaporator giving a reddish oil. The residue oil was purified by column chromatography with CH_2Cl_2 as elutant, yielding the product as a red-brown crystalline solid after removal of solvent. The final products were protected from light.

2.2. Enzyme inhibition assay

Enzyme inhibitory studies were carried out by using Ryan and Ellman method [20] with slight modification. 100 µL of each sample (20, 40, 60, 80, 100 µM) was mixed with 50 µL enzyme (AChE/BChE) and allowed it to stand for 10 min. 50 µL of substrate *i.e.* acetylthiocholine iodide (0.71 mM) for AChE or butyrylthiocholine chloride (0.2 mM) for BChE, 50 µL (0.5 mM) of DTNB [5,5′-dithio-*bis*(2-nitrobenzoic acid)] and 500 µL phosphate buffer of pH 8 added to above mixture and incubated for 20 min at 37 °C. Solution turned yellow due to formation of 5-thio-2-nitrobenzoate anion as a result of hydrolysis of substrate. The hydrolysis of substrate is monitored spectrophotometrically by measuring absorbance at wavelength of 400 nm and 412 nm for AChE and BChE, respectively. Percentage inhibition was calculated by this formula:

$$(\%)\text{Inhibition} = \frac{B - A}{B} \times 100$$

Here A = absorbance of the enzyme with test sample; B = absorbance of enzyme without test sample.

Each experiment was repeated thrice and concordant value was used. IC_{50} value was calculated through simple linear regression. Donepezil was used as reference compound [21].

2.3. Molecular docking studies

Molecular docking studies were performed to predict the interaction of enzyme and ligand. Crystal structure of AChE and BChE was obtained from (RCSB) protein data bank ACD Chemsketch and 3D Pro 12.0 were used for the 3D optimization of given compounds and were saved as SYBYL mol 2 file format. AutoDock Tool v1.5.6 was used for docking, 100 different configurations were optimized. Discovery Studio Visualizer v 4.0 was used for visualization of most potent and best poses of under study compounds [20,21].

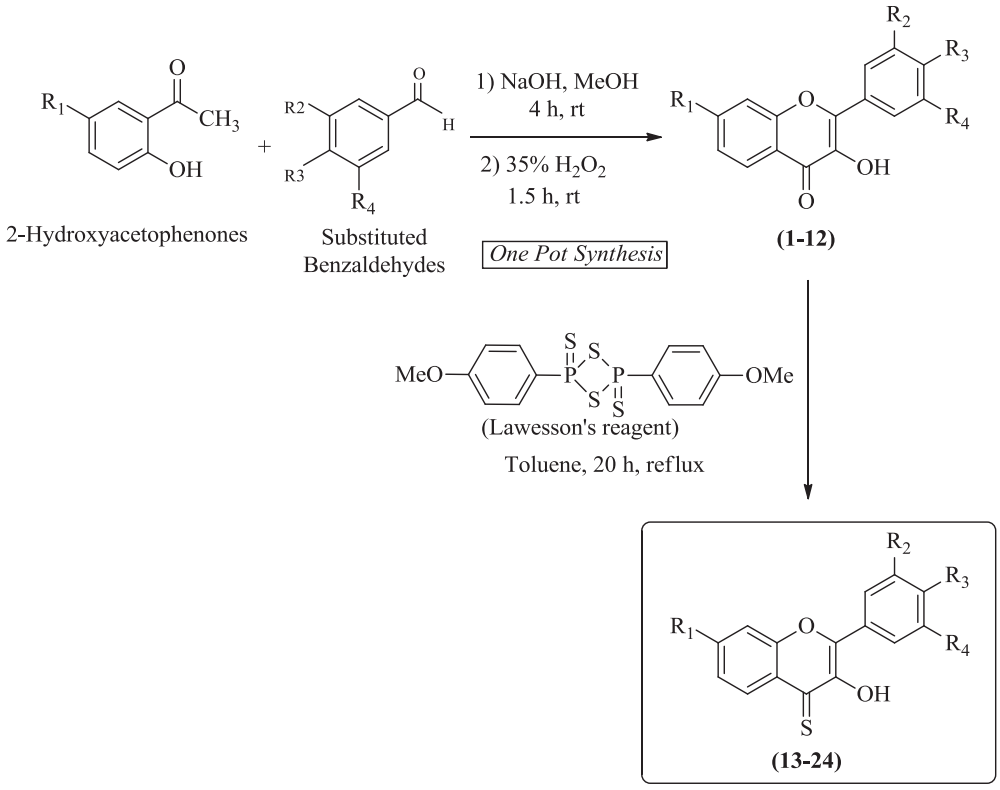

Flavonols	4-Thioflavonols	R_1	R_2	R_3	R_4
1	**13**	H	H	H	H
2	**14**	H	OCH_3	OCH_3	OCH_3
3	**15**	H	H	$N(CH_3)_2$	H
4	**16**	H	H	Cl	H
5	**17**	H	OCH_3	OCH_3	H
6	**18**	H	H	OCH_3	H
7	**19**	H	H	F	H
8	**20**	Br	H	$CH_2CH(CH_3)_2$	H
9	**21**	Br	H	OCH_3	H
10	**22**	H	H	$CH_2CH(CH_3)_2$	H
11	**23**	Br	H	Br	H
12	**24**	Br	H	NO_2	H

Scheme 1. Synthesis of varyingly substituted flavonols (**1–12**) and 4-thioflavonols (**13–24**).

3. Results and discussion

3.1. Chemistry

A series of 3-hydroxyflavones (**1–12**) were synthesized starting from 2-hydroxyacetophenones and varyingly substituted aromatic aldehydes through two-step one-pot literature procedure [21,22], as depicted in Scheme 1.

The base-catalyzed Claisen-Schmidt condensation of 2′-hydroxyacetophenones with various aromatic aldehydes in methanolic solution produced 2′-hydroxychalcones as intermediate compounds. These chalcones were then directly oxidatively cyclized with 30% hydrogen peroxide (H_2O_2), without isolating from the reaction mixture, through well-known Algar-Flynn-Oyamada (AFO) reaction in order to furnish flavonols (**1–12**) in moderate to excellent yields. These compounds were purified through recrystallization by ethanol. Subsequently, flavonols were refluxed with Lawesson's reagent in the presence of anhydrous toluene under inert conditions to afford reddish to brown colored 4-thioflavolnols as crystalline solids in good to excellent yields. These target compounds were purified through silica-gel column chromatography using dichloromethane as eluting solvent. The structures of synthetic 4-thioflavonols (**13–24**) were elucidated by FTIR, NMR spectroscopy and Mass Spectrometry. For instance, in IR spectrum, the disappearance of the C═O signal (1605–1650 cm^{-1}) and appearance of C═S new signal around 1200–1300 cm^{-1} unequivocally confirms the replacement of oxygen by a sulfur atom in the target molecules. This result was further supported by the C═S signal observed in their ^{13}C NMR spectra between 185 and 190 ppm. In addition, ^{1}H spectra show a characteristic singlet between 8 and 9.0 ppm, which corresponds to only one hydroxyl (OH) in the molecules. The molecular masses of the compounds were confirmed by Electron Ionization mass spectrometry (EIMS). Their mass spectra showed the presence of molecular ion peaks as base peaks and give characteristics fragmentation pattern of 4-thioflavonols. All the obtained spectral data were found in full accordance with depicted structures of the newly synthesized compounds.

To the best of our knowledge, the compounds (**1–7**), **9** and **13** are already known, and thus their spectroscopic data can be found in the literature [[23–29] (**1–7** and **9**), 10 (**13**)]. A part from this, all the remaining compounds (**8**, **10–12** and **14–24**) are new. The physico-chemical data of all the newly synthesized compounds are given below:

2-(4-isobutylphenyl)-3-hydroxy-7-bromo-4*H*-chromen-4-one (8)

Yellow crystalline solid; Yield: 92%; m.p. 117–119 °C; UV λ_{max} (CH_2Cl_2) = 325 nm; FTIR (cm^{-1}): 3375, 3064, 1640, 1557, 1465, 1201, 1122; ^{1}H NMR (500 MHz, DMSO-d_6): δ 9.71 (s, 1H, OH), 8.16 (d , J = 5.0 Hz, 1H, Ar-H), 8.02 (d, J = 10.0 Hz, 2H, Ar-H), 7.80 (dd, J = 5.0, 10.0 Hz ,1H, Ar-H), 7.65 (d, J = 5.0 Hz, 1H, Ar-H), 7.25 (d, J = 10.0 Hz, 2H, Ar-H), 2.54 (d, J = 5.0 Hz, 2H, $\underline{CH_2}CH(CH_3)_2$), 1.93–1.89 (m, 1H, $CH_2\underline{CH}(CH_3)_2$), 0.90 (d, J = 5.0 Hz, 6H, $CH_2CH\underline{(CH_3)_2}$) ; ^{13}C NMR (125 MHz, DMSO-d_6): δ 173.0, 154.1, 147.2, 146.1, 14.0, 136.6, 131.4, 130.6, 129.7, 128.0, 127.8, 123.0, 119.7, 45.6 ($-\underline{CH_2}CH(CH_3)_2$), 30.2 ($-CH_2\underline{CH}(CH_3)_2$), 22.5 ($-CH_2CH\underline{(CH_3)_2}$); accurate mass (EI-MS) of $[M]^+$: Calcd. for $C_{19}H_{17}BrO_3$ 372.0361; found 372.0354.

3-hydroxy-2-(4-isobutylphenyl)-4*H*-chromen-4-one (10)

Yellow crystalline solid; Yield: 88%; m.p. 262–265 °C; UV λ_{max} (CH_2Cl_2) = 240 nm; FTIR (cm^{-1}): 3442, 3024, 2910, 1695, 1566, 1490, 1301, 1204, 1198; ^{1}H NMR (500 MHz, DMSO-d_6): δ 9.55 (s, 1H, OH), 8.16–8.11 (m, 3H, Ar-H), 7.83–7.75 (m, 2H, Ar-H), 7.49–7.46 (m, 1H, Ar-H), 7.45–7.34 (m, 2H, Ar-H), 2.53–2.50 (m, 2H, $\underline{CH_2}CH(CH_3)_2$), 1.93–1.85 (m, 1H, $CH_2\underline{CH}(CH_3)_2$), 0.89 (d, J = 5.0 Hz, 6H, $CH_2CH\underline{(CH_3)_2}$); ^{13}C NMR (125 MHz, DMSO-d_6): δ 173.3, 155.0, 146.0, 143.8, 139.2, 134.1, 129.5, 129.2, 128.0, 125.2, 125.0, 121.7, 118.8, (2 carbons are isochrounas), 44.8 ($-\underline{CH_2}CH(CH_3)_2$), 30.0 ($-CH_2\underline{CH}(CH_3)_2$), 22.6 ($-CH_2CH\underline{(CH_3)_2}$); accurate mass (EI-MS) of $[M]^+$: Calcd. for $C_{19}H_{18}O_3$ 294.1255; found 294.1250.

2-(4-bromo-3-hydroxy-7-bromo)-4*H*-chromen-4-one (11)

Light-Yellow solid; Yield: 75%; m.p. 112–115 °C; UV λ_{max} (CH_2Cl_2) = 316 nm; FTIR (cm^{-1}): 3378, 3039, 1638, 1556, 1498, 1342, 1213, 1124; ^{1}H NMR (500 MHz, DMSO-d_6): δ 9.60 (s, 1H, OH), 8.30 (d, J = 5.0 Hz, 1H, Ar-H), 8.10 (d, J = 10.0 Hz, 2H, Ar-H), 7.95–7.83 (m,1H, Ar-H), 7.65 (d, J = 5.0 Hz, 1H, Ar-H), 7.32 (d, J = 10.0 Hz, 2H, Ar-H); ^{13}C NMR (125 MHz, DMSO-d_6): δ 172.7, 160.6, 148.0, 143.8, 142.2, 134.8, 130.6, 130.2, 128.8, 122.0, 121.5, 118.6, 114.5; accurate mass (EI-MS) of $[M]^+$: Calcd. for $C_{15}H_8Br_2O_3$ 393.8840; found 393.8833.

3-hydroxy-2-(4-nitrophenyl)-7-bromo-4*H*-chromen-4-one (12)

Yello solid; Yield: 68%; m.p. 120–122 °C; UV λ_{max} (CH_2Cl_2) = 305 nm; FTIR (cm^{-1}): 3380, 3060, 1645, 1578, 1480, 1330, 1203, 1106; ^{1}H NMR (500 MHz, DMSO-d_6): δ 9.66 (s, 1H, OH), 8.48–8.37 (m, 2H, Ar-H), 7.78 (d, J = 5.0 Hz, 1H, Ar-H), 7.57 (d, J = 10.0 Hz, 1H, Ar-H), 7.46–7.37 (m, 2H, Ar-H), 7.21–7.10 (m, 1H, Ar-H); ^{13}C NMR (125 MHz, DMSO-d_6): δ 174.3, 162.0, 160.8, 156.7, 151.8, 145.4, 144.8, 139.6, 132.7, 129.4, 129.1, 128.3, 128.0, 115.3; accurate mass (EI-MS) of $[M]^+$: Calcd. for $C_{15}H_8BrNO_5$ 360.9585; found 360.9580.

2-(2,3,4-trimethoxy)phenyl)-3-hydroxy-4*H*-chromen-4-thione (14)

Orange crystalline solid; Yield: 77%; m.p. 183–185 °C. UV λ_{max} (CH_2Cl_2) = 372 nm; FTIR

(cm^{-1}): 3415, 3064, 1591, 1552, 1431, 1417, 1274; ^{1}H NMR (500 MHz, $CDCl_3$): δ 8.79 (s, 1H, OH), 8.61–8.57 (m, 1H, Ar-H), 7.73–7.62 (m, 4H, Ar-H), 7.51–7.43 (m, 1H, Ar-H), 3.99 (s, 6H, OMe), 3.97 (s, 3H, OMe); ^{13}CNMR (125 MHz, CD Cl_3): δ 187.3, 174.0, 162.8, 147.4, 144.1, 140.0, 134.1, 126.2, 125.4, 124.1, 115.4, 114.6, 55.4; accurate mass (EI-MS) of $[M]^+$: Calcd. for $C_{18}H_{16}O_5S$ 344.0718; found 344.0710.

2-(4-dimethylamino) phenyl)-3-hydroxy 4*H*-chromen-4-thione (15)

Brigh-purple crystalline solid; Yield: 68%; m.p. 187–189 °C; UV λ_{max} (CH_2Cl_2) = 322 nm; FTIR (cm^{-1}): 3421, 2896, 1608, 1581, 1514, 1375, 1201, 1180; ^{1}H NMR (500 MHz, $CDCl_3$): δ 8.80 (s, 1H, OH), 8.59–8.53 (m , 1H, Ar-H), 8.40 (d, J = 10.0 Hz, 2H, Ar-H), 7.78–7.58 (m, 2H, Ar-H), 7.47–7.40 (m, 1H, Ar-H), 6.68 (d, J = 10.0 Hz, 2H, Ar-H), 3.12 (s, 6H, $N(CH_3)_2$); ^{13}C NMR (125 MHz, $CDCl_3$): δ 189.1, 172.6, 164.3, 163.2, 157.4, 155.7, 152.4, 148.8, 142.8, 136.8, 129.0, 122.8, 116.1, 114.5, 111.3, 38.7; accurate mass (EI-MS) of $[M]^+$: Calcd. for $C_{17}H_{15}NO_2S$ 297.0823; found 297.0817.

3-hydroxy-2-(4-chlorophenyl)-4*H*-chromen-4-thione (16)

Light-orange crystalline solid; Yield: 82%; m.p. 180–181 °C; UV λ_{max} (CH_2Cl_2) = 360 nm; FTIR (cm^{-1}): 3400, 3107, 2920, 1600, 1590, 1487, 1280, 1244; ^{1}H NMR (500 MHz, $CDCl_3$): δ 8.75 (s, 1H, OH), 8.60–8.55 (m, 1H, Ar-H), 8.35 (d, J = 10.0 Hz, 2H, Ar-H), 7.78–7.62 (m, 3H, Ar-H), 7.58 (d, J = 10.0 Hz, 2H, Ar-H); ^{13}C NMR (125 MHz, $CDCl_3$): δ 188.2, 164.8, 162.4, 156.6, 150.2, 147.4, 142.0, 134.3, 131.8, 128.1, 127.4, 120.0, 116.6, 115.2, 114.7; accurate mass (EI-MS) of $[M]^+$: Calcd. for $C_{15}H_9ClO_2S$ 288.0011; found 288.0006.

2-(3, 4-dimethoxy) phenyl)-3-hydroxy-4*H*-chromen-4-thione (17)

Orange crystalline solid; Yield: 75%; m.p. 208–210 °C; UV λ_{max} (CH_2Cl_2) = 452 nm; FTIR (cm^{-1}): 3421, 2999, 2833, 1593, 1517, 1340, 1267, 1226; ^{1}H NMR (500 MHz, $CDCl_3$): δ 8.78 (s, 1H, OH), 8.58–8.53 (m, 1H, Ar-H), 8.05 (dd, J = 5.0, 10.0 Hz, 1H, Ar-H), 8.00 (d, J = 5.0 Hz, 1H, Ar-H), 7.77–7.60 (m, 3H, Ar-H), 7.05 (d, J = 10.0 Hz, 1H, Ar-H), 4.01 (s, 3H, OMe), 3.99 (s, 3H, OMe); ^{13}C NMR (125 MHz, $CDCl_3$): δ 187.2, 173.5, 162.4, 148.0, 144.2, 139.8, 135.0, 126.1, 125.1, 123.8, 115.3, 114.5, 55.3; accurate mass (EI-MS) of $[M]^+$: Calcd. for $C_{17}H_{14}O_4S$ 314.0612; found 314.0602.

2-(4-methoxyphenyl)-3-hydroxy-4*H*-chromen-4-thione (18)

Orange crystalline solid; Yield: 83%; m.p. 208–210 °C; UV λ_{max} (CH_2Cl_2) = 352 nm; FTIR (cm-^{1}): 3418, 3001, 2845, 1590, 1505, 1335,

Table 1
Cholinesterase inhibition efficacy of compounds (**1–24**).

Compound No.	AChE IC_{50} ± SEM[a] (μM)	BChE IC_{50} ± SEM[a] (μM)
1	20.25 ± 0.45	38.15 ± 0.19
2	2.12 ± 0.54	3.21 ± 0.04
3	10.33 ± 0.25	12.36 ± 0.47
4	8.70 ± 0.01	9.01 ± 0.23
5	10.08 ± 0.11	12.23 ± 0.06
6	11.25 ± 0.20	14.00 ± 0.10
7	2 ± 0.45	15.51 ± 0.25
8	1.04 ± 0.03	1.50 ± 0.07
9	10.60 ± 0.03	16.01 ± 0.12
10	2.16 ± 0.76	2.48 ± 0.20
11	2.01 ± 0.36	1.40 ± 0.12
12	12.03 ± 0.15	15.56 ± 0.78
13	2.12 ± 0.04	4.34 ± 0.98
14	1.98 ± 0.11	2.50 ± 0.01
15	13.04 ± 06	15.02 ± 0.78
16	1.15 ± 0.02	3.74 ± 0.03
17	2.38 ± 0.26	4.32 ± 0.85
18	3.00 ± 0.30	3.85 ± 0.25
19	3.25 ± 0.01	4.36 ± 0.06
20	0.08 ± 0.02	0.12 ± 0.08
21	1.23 ± 0.15	2.36 ± 0.64
22	1.96 ± 0.34	3 ± 0.18
23	0.07 ± 0.02	0.15 ± 0.05
24	2.01 ± 0.09	4.50 ± 0.87
Donepezil[St]	0.09 ± 0.01	0.13 ± 0.04

[a] IC_{50} values (mean ± standard error of mean); [St]Standard inhibitor for AChE and BChE enzymes.

1265, 1225; ^{1}H NMR (500 MHz, DMSO-d_6): δ 8.94 (s, 1H, OH), 8.45–8.38 (m, 1H, Ar-H), 8.12 (dd, J = 5.0 , 10.0 Hz, 1H, Ar-H), 8.39 (dd, J = 5.0, 10.0 Hz, 2H, Ar-H), 8.12–8.01 (m, 1H, Ar-H), 7.92–7.88 (m, 1H, Ar-H), 7.48–7.45 (m, 1H, Ar-H), 7.21 (dd, J = 5.0, 10.0 Hz, 2H, Ar-H), 3.89 (s, 3H, OMe); ^{13}C NMR (125 MHz, DMSO-d_6): δ 186.3, 161.0, 155.0, 146.1, 138.8, 134.0, 130.0, 125.5, 124.06, 122.0, 118.8, 118.3, 114.7, 56.0; accurate mass (EI-MS) of $[M]^{+\cdot}$: Calcd. for $C_{16}H_{12}O_3S$ 284.0507; found 284.0500.

2-(4-fluorophenyl)-3-hydroxy-4*H*-chromen-4-one (19)

Red crystalline solid; Yield: 78%; m.p. 120–122 °C; UV λ_{max} (CH_2Cl_2) = 428 nm; FTIR (cm^{-1}): 3410, 2995, 1608, 1596, 1342, 1311, 1301, 1235; ^{1}H NMR (500 MHz, DMSO-d_6): δ 9.02 (s, 1H, OH), 8.45–8.40 (m, 3H, Ar-H), 7.93–7.87 (m, 2H, Ar-H), 7.61–7.58 (m, 1H, Ar-H), 7.51–7.46 (m, 2H, Ar-H); ^{13}C NMR (125 MHz, DMSO-d_6): δ 188.1, 164.8, 162.8, 150.2, 146.4, 141.1, 134.3, 131.88, 131.81, 128.18, 128.10, 127.4, 119.4, 116.63, 116.45; accurate mass (EI-MS) of $[M]^{+\cdot}$: Calcd. for $C_{15}H_9FO_2S$ 272.0307; found 272.0302.

2-(4-isobutylphenyl)-3-hydroxy-7-bromo-4*H*-chromen-4-thione (20)

Bright-red crystalline solid; Yield: 80%; m.p. 194–196 °C; UV λ_{max} (CH_2Cl_2) = 374 nm; FTIR (cm^{-1}): 3415, 3025, 2952, 1586, 1503, 1332, 1264, 1251; ^{1}H NMR (500 MHz, DMSO-d_6): δ 9.03 (s, 1H, OH), 8.50 (d , J = 5.0 Hz, 1H, Ar-H), 8.27 (d, J = 10.0 Hz, 2H, Ar-H), 8.01 (dd, J = 5.0, 10.0 Hz ,1H, Ar-H), 7.90 (d, J = 5.0 Hz, 1H, Ar-H), 7.41 (d, J = 10.0 Hz, 2H, Ar-H), 2.55 (d, J = 5.0 Hz, 2H, $\underline{CH_2}CH(CH_3)_2$), 1.94–1.89 (m, 1H, $CH_2\underline{CH}(CH_3)_2$), 0.90 (d, J = 5.0 Hz, 6H, $CH_2CH\underline{(CH_3)_2}$) ; ^{13}C NMR (125 MHz, DMSO-d_6): δ 186.0, 149.2, 147.0, 145.7, 142.8, 136.3, 130.0, 129.8, 129.4, 129.1, 128.1, 122.1, 119.4, 45.0 ($-\underline{CH_2}CH(CH_3)_2$), 30.0 ($-CH_2\underline{CH}(CH_3)_2$), 22.6 ($-CH_2CH\underline{(CH_3)_2}$); accurate mass (EI-MS) of $[M]^+$: Calcd. for $C_{19}H_{17}BrO_2S$ 388.0132; found 388.0128.

2-(4-methoxyphenyl-3-hydroxy-7-bromo-4*H*-chromen-4-thione (21)

Bright-red crystalline solid; Yield: 86%; m.p. 188–190 °C; UV λ_{max} (CH_2Cl_2) = 438 nm; FTIR (cm^{-1}): 3420, 3029, 2865, 1593, 1507, 1378, 1250, 1220; ^{1}H NMR (500 MHz, DMSO-d_6): δ 9.00 (s, 1H, OH), 8.39–8.15 (m, 3H, Ar-H), 7.93–7.80 (m, 2H, Ar-H), 7.18 (s, 2H, Ar-H), 3.88 (s, 3H, OMe); ^{13}C NMR (125 MHz, DMSO-d_6): δ 184.7, 162.3, 149.1, 146.6, 143.1, 136.1, 131.3, 129.8, 129.3, 122.6, 122.0, 119.3, 115.0, 56.0; accurate mass (EI-MS) of $[M]^{+\cdot}$: Calcd. for $C_{16}H_{11}BrO_3S$ 361.9612; found 361.96102.

3-hydroxy-2-(4-isobutylphenyl)-4*H*-chromen-4-thione (22)

Light-orange crystalline solid; Yield: 82%; m.p. 147–149 °C; UV λ_{max} (CH_2Cl_2) = 380 nm; FTIR (cm^{-1}): 3398, 3080, 2965, 1602, 1527, 1468, 1354, 1250, 1210; ^{1}H NMR (500 MHz, DMSO-d_6): δ 8.95 (s, 1H, OH), 8.45–8.43 (m, 1H, Ar-H), 8.29–8.27 (m, 2H, Ar-H), 7.92–7.86 (m, 2H, Ar-H), 7.60–7.57 (m, 1H, Ar-H), 7.42–7.40 (m, 2H, Ar-H), 2.55 (d, J = 10.0 Hz, 2H, $\underline{CH_2}CH(CH_3)_2$), 1.94–1.88 (m, 1H, $CH_2\underline{CH}(CH_3)_2$), 0.89 (d, J = 5.0 Hz, 6H, $CH_2CH\underline{(CH_3)_2}$);

^{13}C NMR (125 MHz, DMSO-d_6): δ 187.4, 150.2, 146.4, 145.5, 142.3, 134.1, 130.0, 129.0, 128.3, 128.1, 127.9, 126.7, 119.4, 45.0 ($-\underline{CH_2}CH(CH_3)_2$), 30.0 ($-CH_2\underline{CH}(CH_3)_2$), 22.6 ($-CH_2CH\underline{(CH_3)_2}$); accurate mass (EI-MS) of $[M]^{+\cdot}$: Calcd. for $C_{19}H_{18}O_2S$ 310.1027; found 310.1020.

2-(4-bromo-3-hydroxy-7-bromo)-4*H*-chromen-4-thione (23)

Reddish crystalline solid; Yield: 80%; m.p. 183–184 °C; UV λ_{max} (CH_2Cl_2) = 396 nm; FTIR (cm^{-1}): 3414, 3004, 2898, 1598, 1509, 1349, 1285, 1237; ^{1}H NMR (500 MHz, DMSO-d_6): δ 8.89 (s, 1H, OH), 8.45 (d, J = 5.0 Hz, 1H, Ar-H), 8.14 (d, J = 10.0 Hz, 2H, Ar-H), 7.95 (dd, J = 5.0, 10.0 Hz ,1H, Ar-H), 7.70 (d, J = 5.0 Hz, 1H, Ar-H), 7.50 (d, J = 10.0 Hz, 2H, Ar-H); ^{13}C NMR (125 MHz, DMSO-d_6): δ 186.0, 161.8, 148.7, 144.6, 142.0, 135.1, 131.0, 130.0, 129.1, 122.1, 121.7, 118.8, 114.6; accurate mass (EI-MS) of $[M]^{+\cdot}$: Calcd. for $C_{15}H_8Br_2O_2S$ 409.8611; found 409.8601.

3-hydroxy-2-(4-nitrophenyl)-7-bromo-4*H*-chromen-4-thione (24)

Dark-red solid; Yield: 75%; m.p. 180–182 °C; UV λ_{max} (CH_2Cl_2) = 395 nm; FTIR (cm^{-1}): 3435, 3101, 2936, 1603, 1512, 1428, 1326, 1247, 1232; ^{1}H NMR (500 MHz, DMSO-d_6): δ 9.05 (s, 1H, OH), 8.65 (dd, J = 5.0, 10.0 Hz, 2H, Ar-H), 7.95 (d, J = 5.0 Hz, 1H, Ar-H), 7.80 (d, J = 10.0 Hz, 1H, Ar-H), 7.50 (dd, dd, J = 5.0, 10.0 Hz, 2H, Ar-H), 7.42–7.35 (m, 1H, Ar-H); ^{13}C NMR (125 MHz, DMSO-d_6): δ 187.8, 163.2, 161.7, 157.5, 152.4, 146.6, 145.1, 139.7, 133.4, 129.3, 129.0, 128.4, 128.0, 115.4; accurate mass (EI-MS) of $[M]^{+\cdot}$: Calcd. for $C_{15}H_8BrNO_4S$ 376.9357; found 376.9345.

3.2. Cholinesterase enzymes inhibition assay

In continuation to our efforts on cholinesterase enzymes inhibition studies [20,21], all the flavonols (**1–12**) and 4-thioflavonols (**13–24**) were investigated, *in vitro*, for their inhibitory potential against commercially available electric eel acetylcholinesterase (AChE) and horse serum butrylcholinesterase (BChE) enzymes by employing precedent spectrophotometric method. The obtained experimental results were summarized in Table 1. Their IC_{50} values were also calculated, and Donepezil was used as a reference compound.

3.3. Structure-activity relationship

All the tested compounds (**1–24**) exhibited potent varying degree of inhibition (IC_{50} ± SEM = 0.07 ± 0.02 to 15.51 ± 0.25 μM) as compared to the standard drug Donepezil (IC_{50} ± SEM = 0.09 ± 0.01 (AChE) and 0.13 ± 0.04 μM (BChE). Noteworthy, the experimental results revealed that all these compounds are potent selective inhibitors of AChE enzyme. Relatively smaller active site of the AChE enzyme that can assimilate the smaller groups unlike the larger active site of BChE enzyme are accountable for such kind of unique behavior. Notwithstanding that all the structural features are actively taking part in inhibitory activity, however, the variation of different groups on main structural motif was actually accountable for alteration in inhibitory potential. Remarkably, among the series, the compounds **20** (IC_{50} = 0.08 ± 0.02 for AChE and 0.12 ± 0.08 μM for BChE) and **23** (IC_{50} = 0.07 ± 0.02 for AChE and 0.15 ± 0.05 for BChE) were found the most potent dual inhibitors of AChE and BChE enzymes, even more

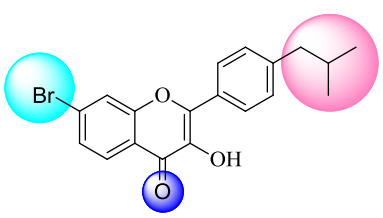

8

AChE (IC_{50} ± SEM) = 1.04±0.03 μM

BChE (IC_{50} ± SEM) = 1.50±0.07 μM

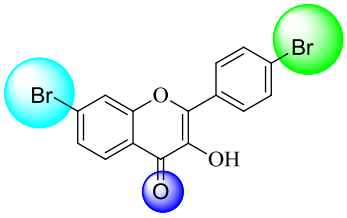

11

AChE (IC_{50} ± SEM) = 2.01±0.36 μM

BChE (IC_{50} ± SEM) = 1.40±0.12 μM

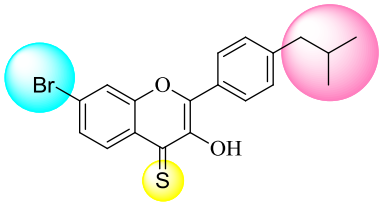

20

AChE (IC_{50} ± SEM) = 0.08±0.02 μM

BChE (IC_{50} ± SEM) = 0.12±0.08 μM

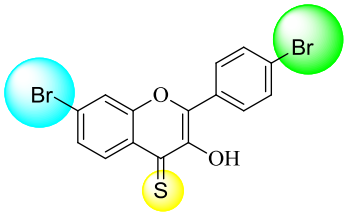

23

AChE (IC_{50} ± SEM) = 0.07±0.02 μM

BChE (IC_{50} ± SEM) = 0.15±0.05 μM

Fig. 2. Structure-activity relationship of the most potent compounds.

active than standard Donepezil drug (Fig. 2). However, these both compounds are comparatively more active against AChE than BChE (Table 1). The compound **20** has bromo group at position-7 in ring A and isobutyl at 4′ position in ring B of the flavonol carbon framework. The high inhibitory potential of this compound is mainly due to hydrophobic interactions of that alkyl group with non-polar pockets and strong polar interactions with polar active pockets of the envisioned enzymes.

Moreover, the other most potent dual inhibitor is compound **23** (IC_{50} = 0.07 ± 0.02 μM for AChE and 0.15 ± 0.05 μM for BChE) having one bromo group at 7-position of the ring A and other bromo group at 4′ position of the ring B. Its inhibitory potential is due to the formation of strong non-bonding interactions with active pockets of the envisioned enzymes. In addition, the next most potent dual inhibitors were the oxygen analogues (the compounds **8** and **11**) of the compounds **20** and **23**. Their structural pattern is similar to that of sulfur analogs (**20** and **23**) (Fig. 2). Because of this fact, their interactions towards the AChE and BChE enzymes are also similar to the derivatives **20** and **23**. However, they have strong interactions with previously mentioned enzymes owing to the relatively better coordination of sulfur than oxygen. It is noteworthy that the compound **11** was found the selective inhibitor of BChE amongst the whole series. Probably, it nicely fits into the active pockets of BChE, and thus has stable and substantial interactions with it.

Furthermore, the simple flavonol derivative was appeared to be about least inhibitor against both enzymes among the series (Table 1). However, its sulfur analogue **13** has relatively more inhibitory activity against AChE and BChE. Interestingly, it has been noticed that 4-thioflavonols (**13–24**) are comparatively better inhibitor against AChE as compared to BChE (Table 1). These findings could be attributed to the better coordinating properties of sulfur than oxygen. 4-thioflavonols make significant interactions with the active sites of both enzymes. However, overall, all the synthetic derivatives (**1–24**) are found to be selective inhibitor of AChE. The obtained results displayed that the nature and pattern of substitution at both rings A and B enhance inhibitory potential of these compounds against both the envisioned enzymes. Since, all the intended compounds have common 3-hydroxyflavone skeleton in their structures; the inhibitory potential of these compounds appears to be purely due to the presence of different substituents at various positions of the main 3-hydroxyflavone scaffold as well as thio-keto group in 4-thioflavonols. Both factors are accountable to raise the inhibitory activity of these planned compounds (**1–24**). Furthermore, in addition to the compounds **20** and **23**, the remaining derivatives were found as either selective inhibitors of acetylcholinesterase or have shown dual inhibition towards both the enzymes. These experimental results were further supported by *in silico* computational studies (molecular docking). Based on these results, 4-thioflavonols with multiple functionalities could pave the way for designing and the development of new structural motifs for the cure of Alzheimer disease.

3.4. Molecular docking studies

In order to validate the experimental results and to find out plausible binding interactions of inhibitors with the active pocket sizes of the proposed enzymes, the molecular docking studies were performed. Also, these theoretical studies were planned to figure out protein–ligand interactions at molecular level for establishing SAR studies. In this context, X-ray structures of human AChE (PDB ID: 4BDT) and BChE (PDB ID: 4BDS) were selected as templates. The lowest bonding energies of the compounds (**1–24**) obtained after docking analysis are given in the Table 2.

The results *in vitro* clarified the most potent derivative is compound **20** even more active than standard drug. This ligand inherits the inhibition capabilities against AChE via numerous kinds of interactions, such as it associates with the TRP86 and TYR337 of catalytic triad amino acid residues via hydrophobic pi-pi stacked and hydrophobic pi-alkyl type of attractive forces respectively. SER125, GLU202, MET443, PRO446, TYR449 amino acid residues of AChE possess the pi-donor hydrogen bond, conventional hydrogen bond, hydrophobic alkyl and

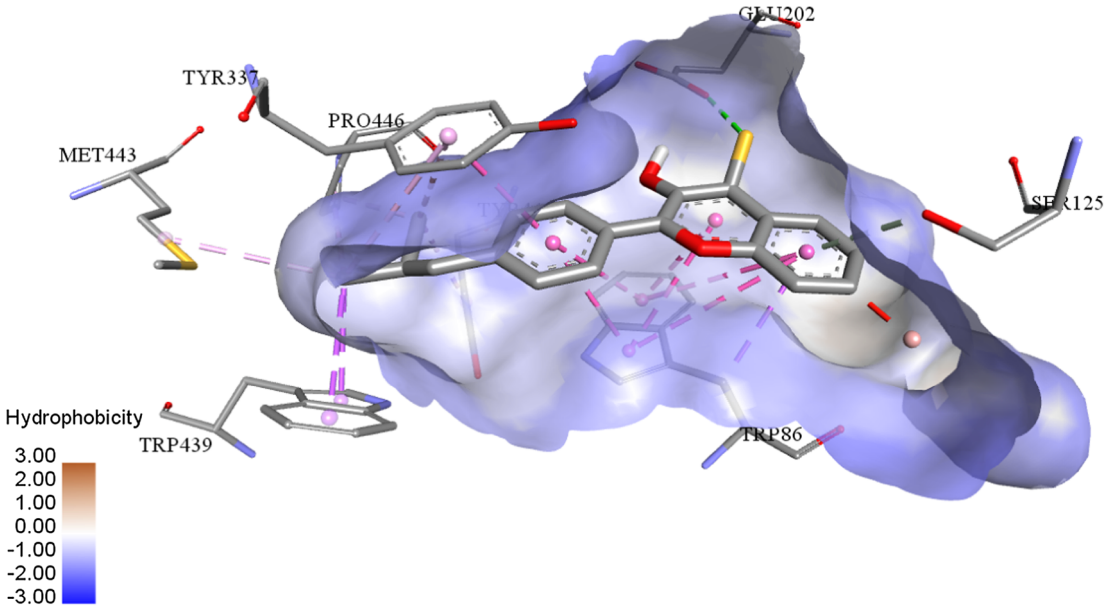

Fig. 3. Putative binding interactions of compound **20** against AChE.

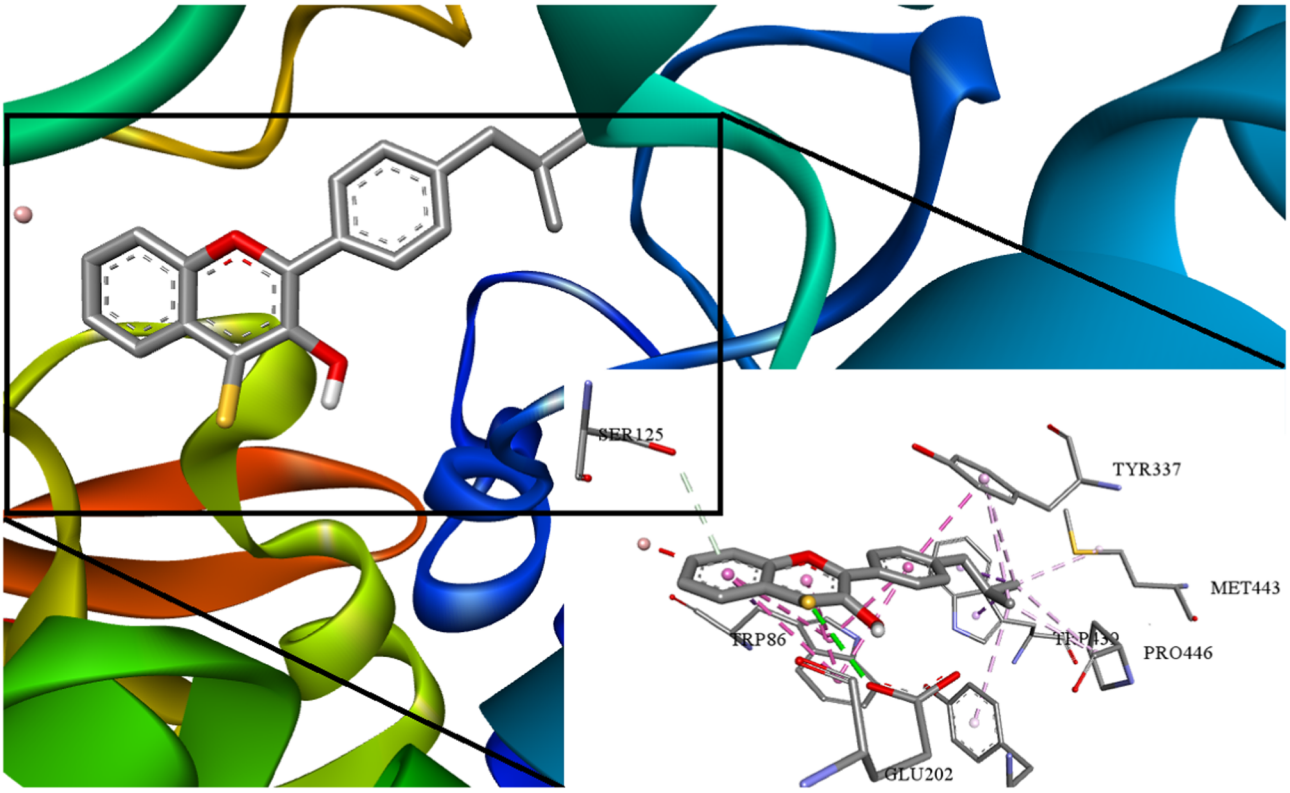

Fig. 4. Interactions of the compound **20** with AChE at 3D space. Interactions with specific amino acid residues are shown in the box. The 3D ribbon represents the enzyme-stick model is the lowest energy conforms of the inhibitor **20** along with amino acids of AChE interacting with it.

hydrophobic pi-alkyl type of interactions with the ligand **20** inside the pocket of AChE as diagrammatically elaborated in Figs. 3 and 4.

Similarly, this ligand shows its inhibitory potential inside the active pockets of BChE by developing conventional hydrogen bonding with GLU197 and SER198 of oxyanion hole. TRP 82 of peripheral anion site (PAS) exhibit hydrophobic pi-pi *T*-shaped type association with this ligand inside BChE. ALA328, PHE329, LEU286, VAL288, TRP231, PHE398 also possess the hydrophobic pi-alkyl, hydrophobic alkyl and hydrophobic pi-sigma types bonding with the compound **20** inside BChE as shown in Figs. 5 and 6.

Furthermore, another the most potent dual inhibitor of AChE and BChE was the derivative **23**. This ligand also unveils its inhibitory potential against AChE via numerous types of linkages. It uses all of its three rings A, B and C to form hydrophobic pi-pi stacked interaction with the catalytic triad amino acid residues TRP86 and TYR337 inside the active pockets of AChE. It also uses its OH group at C-3 for hydrogen bonding with HIS447 inside the AChE as depicted in Figs. 7 and 8.

In the same way, theoretical studies of compound **23** reveals its

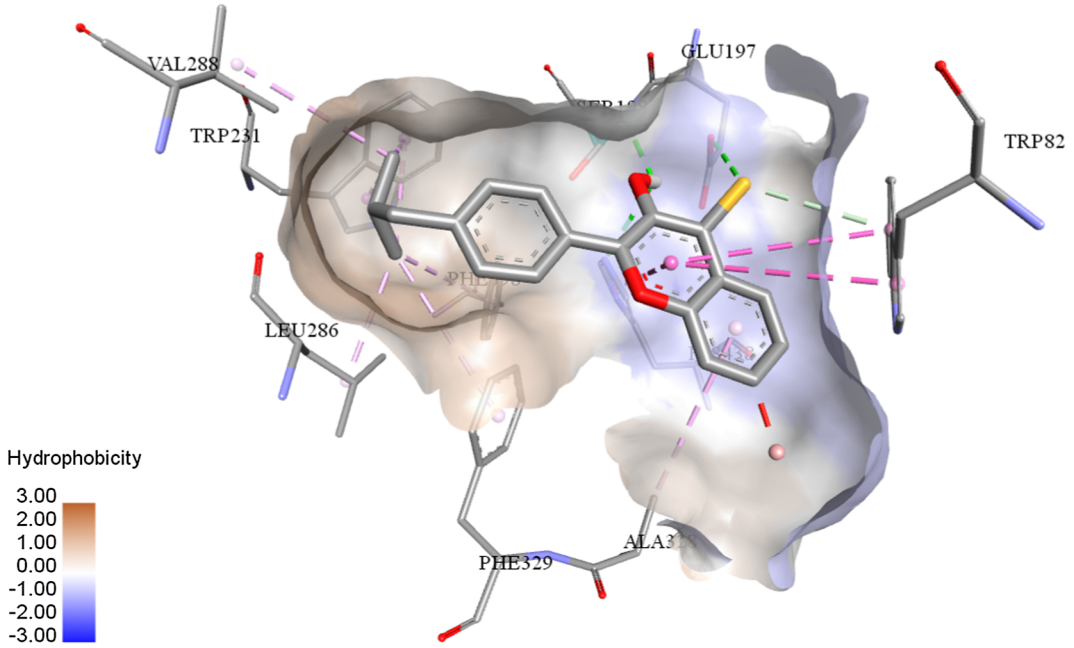

Fig. 5. Putative binding interactions of compound **20** against BChE.

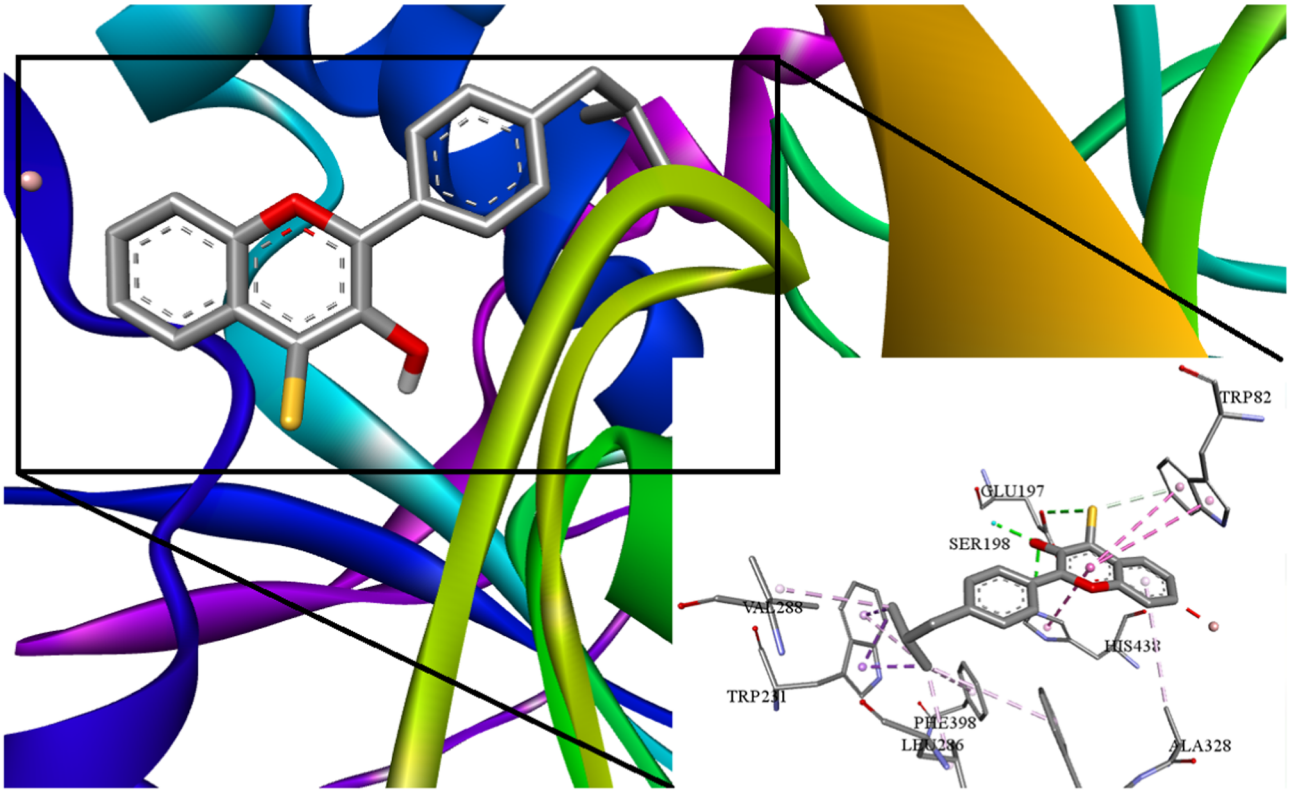

Fig. 6. Interactions of the compound **20** with BChE at 3D space. Interactions with specific amino acid residues are shown in the box. The 3D ribbon represents the enzyme-stick model is the lowest energy conforms of the inhibitor **20** along with amino acids of BChE interacting with it.

inhibition potential against BChE. Heterocyclic ring and thio-keto group of this ligand develops hydrophobic pi-pi *T*-shaped and pi-sulphur type interactions with the TRP82 of peripheral anionic site residue (PAS) inside BChE. SER198 shows hydrogen bonding with this ligand inside the active pocket of BChE. This ligand also possesses the hydrophobic pi-alkyl, hydrophobic pi-pi *T*-shaped and hydrogen bonding type interactions with ALA328, HIS438, GLU197 inside the active pockets of BChE as displayed in Figs. 9 and 10.

Thus, these terrific and robust interactions anchored the derivative **20** and derivative **23** and, helped them in stabilizing in the active site of the receptors. The derivatives **20** and **23** showed promising binding energies -10.09 KJ mol^{-1} and -10.20 KJ mol^{-1} for AChE and, -9.80 KJ mol^{-1} and -9.41 KJ mol^{-1} for BChE, respectively (Table 2) which can be accredited to observed interactions. Results of the docking simulations are quite consistent with the experimental finding. Hence good acetylcholinesterase and butyrylcholinesterase activities with

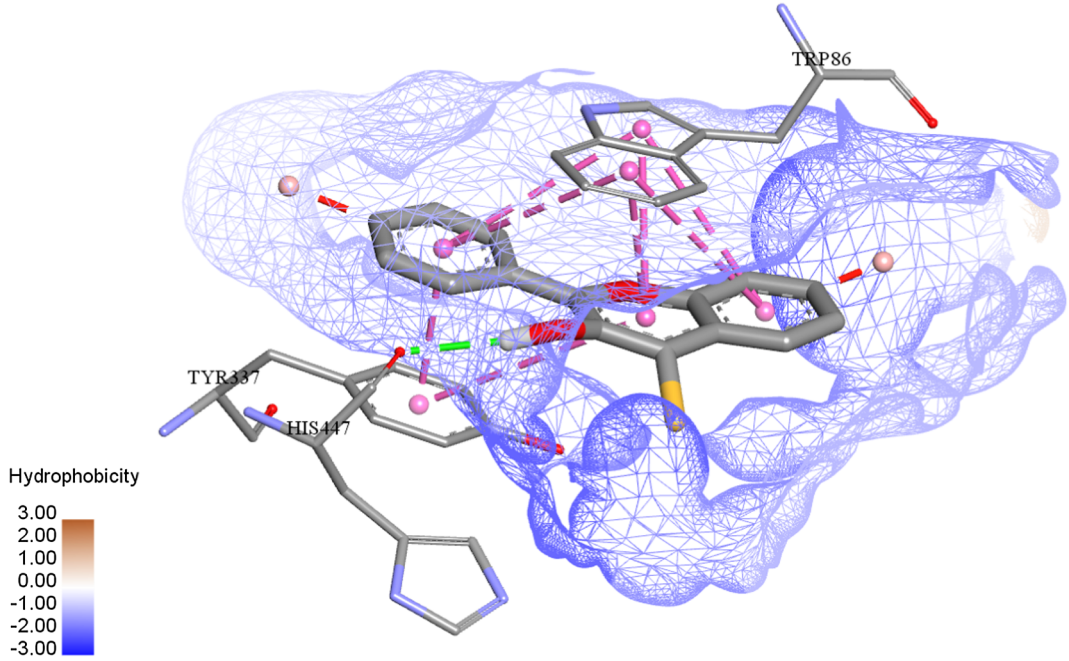

Fig. 7. Putative binding interactions of compound **23** against AChE.

lowest IC 50 values (Table 1) of derivative **20** and derivative **23** can be accredited to their good binding energies and tremendous interactions with key amino acids. These striking interactions and binding energies suggest that the derivative **20** and derivative **23** possess the strong potential to influence the catalytic activities of the enzyme and can act as a potential surrogate for the development of novel acetylcholinesterase and butyrylcholinesterase inhibitors.

4. Conclusions

In summary, we have designed and synthesized a fascinating series of flavonol derivatives, bearing diverse substitution pattern, by employing precedent methodologies. These compounds were then efficiently chemically transformed into 4-thioflavonols by using Lawesson's reagent as thionating agent, and also successfully characterized by

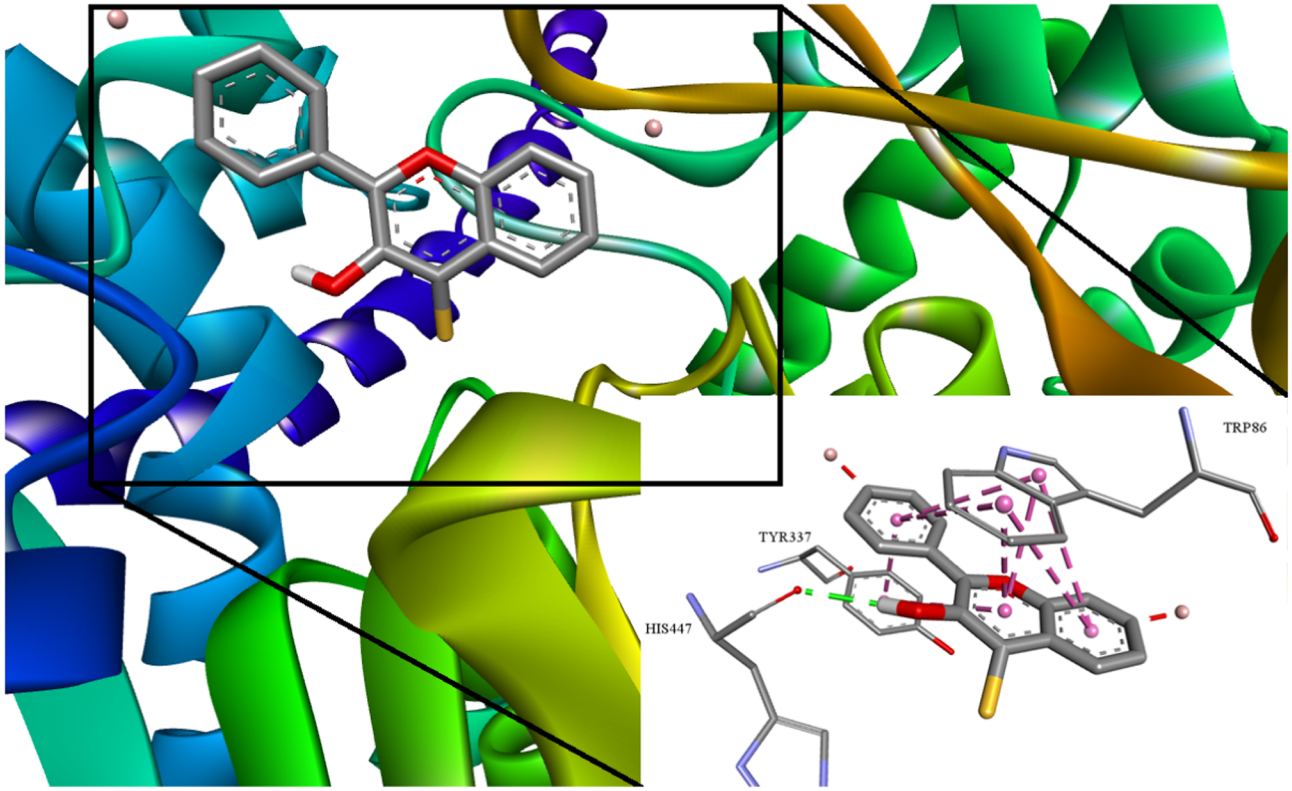

Fig. 8. Interactions of the compound **23** with AChE at 3D space. Interactions with specific amino acid residues are shown in the box. The 3D ribbon represents the enzyme-stick model is the lowest energy conforms of the inhibitor **23** along with amino acids of AChE interacting with it.

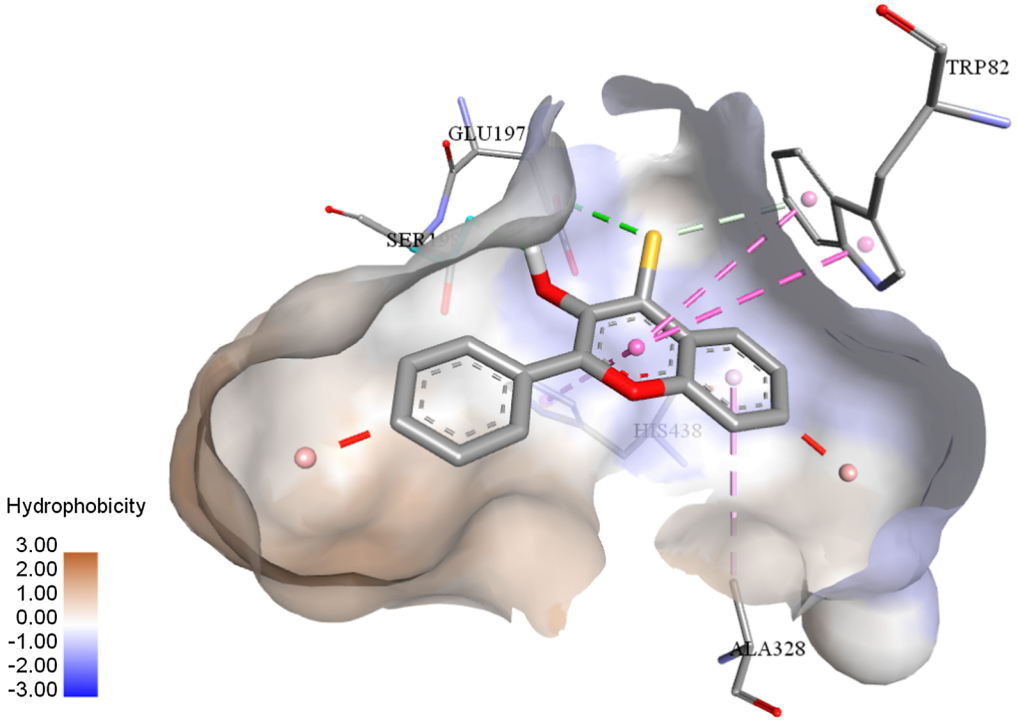

Fig. 9. Putative binding interactions of compound **23** against BChE.

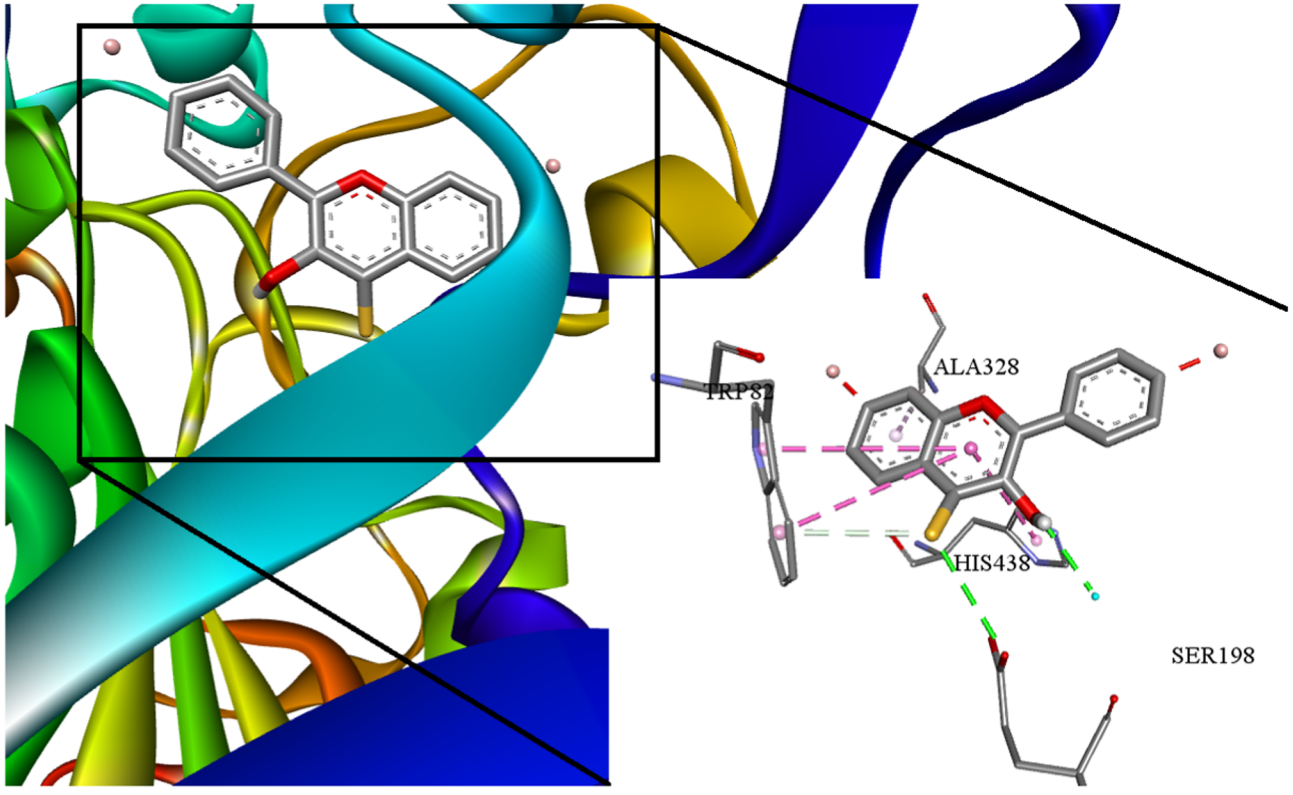

Fig. 10. Interactions of the compound **23** with BChE at 3D space. Interactions with specific amino acid residues are shown in the box. The 3D ribbon represents the enzyme-stick model is the lowest energy conforms of the inhibitor **23** along with amino acids of BChE interacting with it.

usual spectroscopic techniques. All these compounds (**1–24**) were screened for their inhibitory potential against AChE and BChE enzymes. The results revealed that all the investigated compounds were selective inhibitors of AChE except the compound **11**, which was selective inhibitor of BChE. Moreover, enzymes inhibition assay showed that thio-analogues (**13–24**) were comparatively more active than their precursors (**1–12**). This is attributed to the better co-ordination of sulfur atom than oxygen. Notably, the derivatives **20** and **23** were found highly potent as nearly dual inhibitors of AChE and BChE among the whole series, even more active than Donepezil. Also, the SAR studies

Table 2
Binding energies of selective modes against human AChE and BChE enzymes.

Compound No.	*h* AChE Lowest Binding Energy ΔG in KJ mol^{-1}	*h* BChE Lowest Binding Energy ΔG in KJ mol^{-1}
1	−8.31	−7.95
2	−9.22	−9.04
3	−8.38	−8.41
4	−8.80	−8.51
5	−8.35	−8.34
6	−8.54	−8.15
7	−8.43	−7.84
8	−9.40	−9.10
9	−8.66	−8.32
10	−9.06	−9.47
11	−9.00	−9.84
12	−8.24	−8.23
13	−9.15	−8.66
14	−9.63	−9.39
15	−8.94	−8.84
16	−9.54	−9.05
17	−9.38	−8.88
18	−9.14	−9.01
19	−9.16	−8.57
20	−10.09	−9.80
21	−9.66	−8.82
22	−9.88	−9.16
23	−10.20	−9.41
24	−9.20	−8.76
Standard	−10 (HUW)	−6.83 (THA)

were established on the basis of substitution pattern on flavonol structure as well as keto-and thioketo- groups. The experimental results were further supported by molecular docking analysis. The computational results were in good agreement with the experimental results. On the basis of above-mentioned findings, new scaffolds could be envisioned and developed for the treatment of Alzheimer disease. We are quite confident that these results may be of interest for applications in medicinal/pharmaceutical chemistry.

Acknowledgements

We are highly thankful to Prof. Dr. Norbert Sewald, Department of Organic Chemistry III, Bielefeld University, Germany for his kind help in spectroscopic measurements. The financial support for this work is also gratefully acknowledged by Higher Education Commission of Pakistan under the NRPU Project No. 6484.

References

[1] (a) D. Seleem, V. Pardi, R.M. Murata, Arch. Oral Biol. 76 (2017) 76–83;
(b) A. Singh, S. Kumar, V. Bajpai, T.J. Reddy, K.B. Rameshkumar, B. Kumar, Rapid Commun. Mass Spectrom. 29 (12) (2015) 1095–1106;
(c) T.-D. Tran, T.-C.-V. Nguyen, N.-S. Nguyen, D.-M. Nguyen, T.-T.-H. Nguyen, M.-T. Le, K.-M. Thai, Appl. Sci. 6 (7) (2016) 198;
(d) X. Shen, Q. Zhou, W. Xiong, W. Pu, W. Zhang, G. Zhang, C. Wang, Tetrahedron 73 (32) (2017) 4822–4829.
[2] B. Butun, G. Topcu, T. Ozturk, Mini-Rev. Med. Chem. 18 (2) (2018) 98–103.
[3] R.G. Britton, E. Horner-Glister, O.A. Pomenya, E.E. Smith, R. Denton, P.R. Jenkins, W.P. Steward, K. Brown, A. Gescher, S. Sale, Eur. J. Med. Chem. 54 (2012) 952–958.
[4] M. Gharpure, R. Choudhary, V. Ingle, H. Juneja, ChemInform 44 (2013) 44.
[5] V. Sendrayaperumal, S.I. Pillai, S. Subramanian, Chem. Biol. Interact. 219 (2014) 9–17.
[6] B. Culhaoglu, A. Capan, M. Boga, M. Ozturk, T. Ozturk, G. Topcu, Med. Chem. 13 (3) (2017) 254–259.
[7] T. Murai, Top. Curr. Chem. 376 (4) (2018) 31.
[8] W. Li, P. Han, S. Cai, Q. Wang, Nat. Prod. Res. 27 (2018) 1–6.
[9] I.L. Martins, C. Charneira, V. Gandin, J.L.F.D. Silva, G.C. Justino, J.P. Telo, A.J.S.C. Vieira, C. Marzano, A.M.M. Antunes, J. Med. Chem. 58 (10) (2015) 4250–4265.
[10] B.L. Tran, S.M. Cohen, Chem. Commun. 37 (2006) 203–205.
[11] J. Dong, Q. Zhang, Q. Meng, Z. Wang, S. Li, J. Cui, Mini-Rev. Med. Chem. 18 (20) (2018) 1714–1732.
[12] E.U. Mughal, M. Ayaz, Z. Hussain, A. Hasan, A. Sadiq, M. Riaz, A. Malik, S. Hussain, M.I. Choudhary, Bioorg. Med. Chem. 14 (14) (2006) 4704–4711.
[13] M.T.H. Khan, I. Orhan, F. Şenol, M. Kartal, B. Şener, M. Dvorská, K. Šmejkal, T. Šlapetová, Chem. Biol. Interact. 181 (3) (2009) 383–389.
[14] Y. Shen, J. Zhang, R. Sheng, X. Dong, Q. He, B. Yang, Y. Hu, J. Enzyme Inhib. Med. Chem. 24 (2) (2009) 372–380.
[15] J.Y. Kim, W.S. Lee, Y.S. Kim, M.J. Curtis-Long, B.W. Lee, Y.B. Ryu, K.H. Park, J. Agric. Food. Chem. 59 (9) (2011) 4589–4596.
[16] P. Anand, B. Singh, Arch. Pharmacal. Res. 36 (4) (2013) 375–399.
[17] M. Jung, M. Park, Molecules 12 (9) (2007) 2130–2139.
[18] M. Bakhtiari, Y. Panahi, J. Ameli, B. Darvishi, Biomed. Pharmacother. 93 (2017) 218–229.
[19] M. Katalinić, G. Rusak, J.D. Barović, G. Šinko, D. Jelić, R. Antolović, Z. Kovarik, Eur. J. Med. Chem. 45 (1) (2010) 186–192.
[20] (a) E.U. Mughal, A. Sadiq, S. Murtaza, H. Rafique, M.N. Zafar, T. Riaz, B.A. Khan, A. Hameed, K.M. Khan, Bioorg. Med. Chem. 25 (1) (2017) 100–106;
(b) E.U. Mughal, A. Sadiq, B.A. Khan, M.N. Zafar, I. Ahmed, M. Zubair, Lett. Drug Des. Discov. 14 (9) (2017) 1035–1041.
[21] E.U. Mughal, A. Javid, A. Sadiq, S. Murtaza, M.N. Zafar, B.A. Khan, S.H. Sumrra, M.N. Tahir, Kanwal, K.M. Khan, Bioorg. Med. Chem. 26 (13) (2018) 3696–3706.
[22] X. Li, M. Lee, G. Chen, Q. Zhang, S. Zheng, G. Wang, Q.-H. Chen, Bioorg. Med. Chem. 25 (17) (2017) 4768–4777.
[23] D. Brondani, I.C. Vieira, C. Piovezan, J.M.R. da Silva, A. Neves, J. Dupont, C.W. Scheeren, Sensor for fisetin based on gold nanoparticles in ionic liquid and binuclear nickel complex immobilized in silica, Analyst 135 (5) (2010) 1015–1022.
[24] C.K. Hill, S.E. Saad, R.G. Britton, A.J. Gescher, S. Sale, K. Brown, L.M. Howells, Inhibition of prostate cancer cell growth by 3′, 4′, 5′-trimethoxyflavonol (TMFol), Cancer Chemother. Pharmacol. 76 (1) (2015) 179–185.
[25] V.G. Pivovarenko, O.B. Vadzyuk, S.O. Kosterin, Fluorometric detection of adenosine triphosphate with 3-hydroxy-4′-(dimethylamino) flavone in aqueous solutions, J. Fluoresc. 16 (1) (2006) 9–15.
[26] K. Afarinkia, A.T. Balaban, T.S. Balaban, N. Camp, S. Faulkner, Science of Synthesis: Houben-Weyl Methods of Molecular Transformations Vol. 14: Six-Membered Hetarenes with One Chalcogen. Georg Thieme Verlag, 2014.
[27] J. Gowan, P. Hayden, T. Wheeler, A new synthesis of flavonols, J. Chem. Soc. (Resumed) (1955) 862–866.
[28] N. Pogodaeva, B. Sukhov, S. Medvedeva, Enantioselective keto-enol tautomerism of 3-hydroxyflavones upon molecular complex formation of their α-Diketo forms with carbohydrates in aqueous solutions, Chem. Nat. Compd. 52 (4) (2016) 579–584.
[29] V.S. Dofe, A.P. Sarkate, D.K. Lokwani, S.H. Kathwate, C.H. Gill, Synthesis, anti-microbial evaluation, and molecular docking studies of novel chromone based 1, 2, 3-triazoles, Res. Chem. Intermed. 43 (1) (2017) 15–28.